Tracking Spectroscopically Determined H-alpha and H-beta Indices for Two Emission-Line Objects

Tyler B. Harding
Eric G. Hintz
Department of Physics and Astronomy, Brigham Young University, Provo, UT 84602; hintz@byu.edu

Received July 29, 2022; revised February 16, May 11, July 5, 2023, accepted July 5, 2023

Abstract Spectroscopic methods were used to monitor the Hα and Hβ indices for two emission-line objects, X Persei and γ Cassiopeiae. The spectroscopic data covered a timeline from 2010 to 2020. The Hα index for X Per showed substantial variation, with the Hβ index changes being less pronounced. The shape of the Hα variations for X Per were a mirror image to archival V-magnitude observations. In the case of γ Cas only a slight rise in value for the Hα index was seen. To allow comparison to published observations, we determined a transformation from the two indices to equivalent width values. The values determined for X Per fill time gaps in the previously published equivalent width values. The γ Cas values provide no additional coverage.

1. Introduction

Joner and Hintz (2015) detail calibrated Hα and Hβ indices for a significant number of main sequence stars. The Hβ index is effectively the original photometric filter system designed by Crawford (1960) and often used in conjunction with the Strömgren filter set. The index is based on wide and narrow filters centered on the Hβ line. Although not stated in Joner and Hintz (2015), the development of a similar Hα index started with the creation of similar physical filters centered on the Hα line. To check the early results a set of spectroscopic observations was obtained. This allowed testing of a range of filter shapes since different functions could be convolved over the spectrum to obtain photometric values. The development of the new Hα index then became a photometric project based on spectroscopic observations. However, in the end scans of the original filters were used to determine the values that appear in Joner and Hintz (2015).

As part of the observing program that led to Joner and Hintz (2015), data were secured for a wide range of potentially variable objects such as pulsating variable stars Bugg and Hintz (2019), eclipsing binaries, active galaxies, and emission-line objects. This was in preparation for the potential long-term monitoring with physical filters. Two of the emission-line objects observed were X Persei (X Per) and γ Cassiopeiae (γ Cas). Here we will demonstrate the ability of the two indices to track temporal changes of spectral lines for these types of objects.

While the indices can be used to monitor changes in emission line strength on their own, we recognize the need to compare with published equivalent width measurements (EW hereafter). Therefore, we provide a calibrated conversion of the Hα and Hβ indices to EW values. For comparison we gathered EW values for X Per from a number of papers (Roche *et al.* 1993; Engin and Yuce 1998; Liu and Hang 2001; Grundstrom *et al.* 2007; Li *et al.* 2014; Reig *et al.* 2016; Zamanov *et al.* 2019). This provides nearly continuous coverage from 1979 to 2021 for at least the Hα line. A good summary of recent Hα EW measurements for γ Cas was found in Pollmann (2021).

While the original Joner and Hintz (2015) paper was based on scanned filter functions convolved over spectroscopic observations, the original intent of the system was to be a photometric system using filters like the original Hβ system. This paper demonstrates the future application of physical filters to monitor variable objects such as emission-line objects.

2. Observations

Spectroscopic data were collected using the 1.2-meter McKellar Telescope of the Dominion Astrophysical Observatory (DAO) operating in robotic mode. Since both targets are the brightest objects in their fields this mode works extremely well and allowed for the collection of a significant number of observations. The observations of X Per were collected from 2010 to 2020, providing 66 total nights of data. A total of 87 nights of data were collected for γ Cas from 2011 to 2020. In addition, spectroscopic observations of 15 other emission-line objects were secured during this same window of time. Each night also contained a sample of the standard stars from Joner and Hintz (2015).

The 3231 grating was used and provided 40.9 Å mm^{-1}. The spectra were imaged onto the Site4 CCD with 15 μm pixels that resulted in a spectral resolution of 0.614 Å $pixel^{-1}$. The Site4 CCD has 4096 pixels along the dispersion axis which provided approximately 2500 Å of total spectral coverage. This grating was aligned to provide a central wavelength of 5710 Å, thus covering a range from 4450 Å to 6970 Å. The selected range allowed for the simultaneous observation of both the Hα and the Hβ lines. All spectra were processed using a FeAr comparison lamp and compressed to 1D using the SPECRED packages in the IRAF reduction software. Figure 1 shows an example processed spectrum for X Per and Figure 2 for γ Cas.

For comparison purposes, V-filter observations of both targets were downloaded from the American Association of Variable Star Observers (hereafter AAVSO) website (Kafka (2021). The AAVSO archive provided 139 data points for X Per for the years 2010 through 2020 and 584 data points for γ Cas for the years 2011 through 2020. It should be noted that more data exist in the AAVSO archive, but we only selected the data which correspond to our timeline.

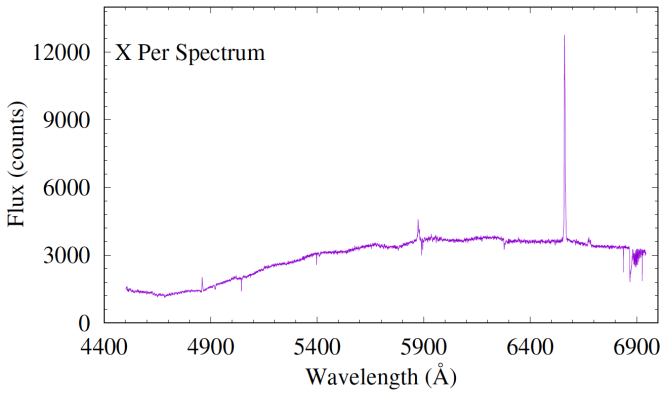

Figure 1. Typical spectrum for X Per collected from the DAO 1.2-m telescope.

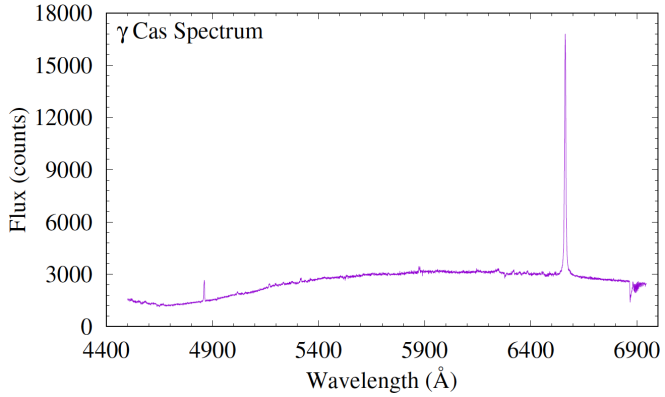

Figure 2. Typical spectrum for γ Cas collected from the DAO 1.2-m telescope.

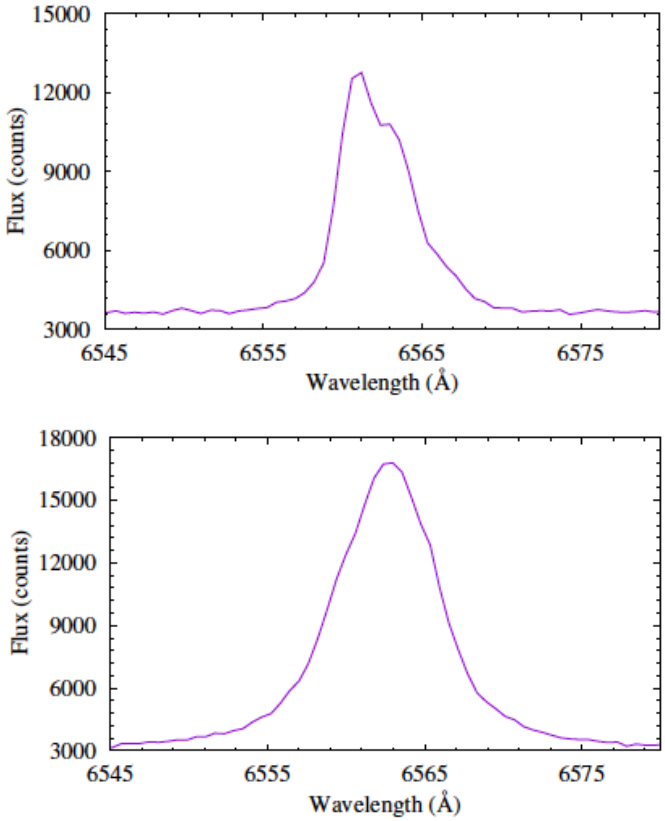

Figure 3. A zoomed in view of the Hα emission line for X Per (top) and γ Cas (bottom).

3. Analysis

After the data were processed to 1D wavelength calibrated spectra, we used the methods detailed in Joner and Hintz (2015) to provide calibrated Hα and Hβ index values for each observation. In other words, we convolved each filter function over the spectrum and formed each index by subtracting the wide magnitude from the narrow magnitude. That value was then calibrated against the standard stars from Joner and Hintz (2015) taken each night.

In Figure 3 we show detailed views of a typical Hα line for X Per and γ Cas. In total we obtained 161 spectra for X Per and 543 spectra for γ Cas. Given that both targets are bright, the error per observation is in the 0.003 to 0.006 range for index measurements. We do note that for some spectra the Hα line was saturated so that we could only determine an Hβ measurement from those spectra. In addition, a number of nights had very low signal in the blue region and the Hβ values were unreliable.

As has been stated before, the Hα and Hβ values were always meant to be done by imaging with physical filters. Since emission-line objects are most often tracked with changes to the EW, we developed a transformation from the index values to EW. To do this we used single observations for 16 emission-line objects mentioned earlier for which we had determined Hα and Hβ indices. Using the SPLOT command within IRAF we examined the EW values. We note that there are five different options for measuring EW with this command. We selected the option that provides the integration of pixel intensities between the marked points (the "e" keystroke). The limits were determined by finding the continuum level then marking the first point where the curve reached this level on each side of the line center. The values are reported in Table 1.

Figure 4 shows the comparison of the index values and the EW values for the Hα line. Both linear and second-order fits were determined. For Hα the coefficients on the second-order fit are clearly significant as shown in Equation 1. In Figure 4 we show the linear fit as a solid line and the second-order fit as a dashed line. The standard errors for the fits are found to be 1.40 Å for the linear fit and 0.60 Å for the second-order fit.

$$EW\alpha = -19.51(2.80)\times H\alpha^2 + 132.70(12.15)\times H\alpha - 211.69(12.99) \quad (1)$$

In Figure 5 the relation between EW and Hβ is displayed. We note that for the Hβ relation HD 31293 was clearly in absorption. Therefore HD 31293 was removed from the transformation discussed here. Again we checked both a linear fit and a second-order fit. A t-test on the second-order terms is right at the edge of significance and the difference in standard error is not significantly improved by inclusion of the second-order term. Therefore, the Hβ to EW transformation is done with a linear fit as given in Equation 2. The error for this transformation is 0.67 Å.

$$EW\beta = 40.07(2.01) \times H\beta - 100.81(4.97) \quad (2)$$

Equation 1 and Equation 2 were used to generate EW values for all our observations. To check the Hα EW values we gathered the published data from HJD 2455000 to HJD 2458500 to match

Table 1. Hα and Hβ versus equivalent width values for a sample of emission-line targets.

Object	*Hα*	*EWα Å*	*Hβ*	*EWβ Å*
κ Dra	2.165	–15.82	2.586	2.32
1H 1936+541	1.995	–23.81	2.493	–2.38
V1357 Cyg	2.549	–0.51	2.554	1.12
λ Cep	2.538	–0.14	2.545	1.25
AG Dra	1.737	–39.48	2.191	–13.95
1H 2202+501	1.770	–38.86	2.532	0.32
4U 2206+54	2.525	–0.76	2.552	1.12
52 Aql	2.405	–6.05	2.520	0.66
α Cam	2.496	–2.29	2.524	0.84
HD 229221	1.934	–27.86	2.424	–3.03
X Per	1.953	–26.93	2.400	–3.82
HD 31293	2.077	–21.43	2.780	14.03
RX J0440.9+4431	2.267	–11.08	2.480	–1.22
EXO 051910+3737.7	1.902	–30.54	2.414	–3.04
1A 0535+262	2.216	–12.48	2.456	–1.93
4U 0548+29	1.828	–33.77	2.466	–2.48

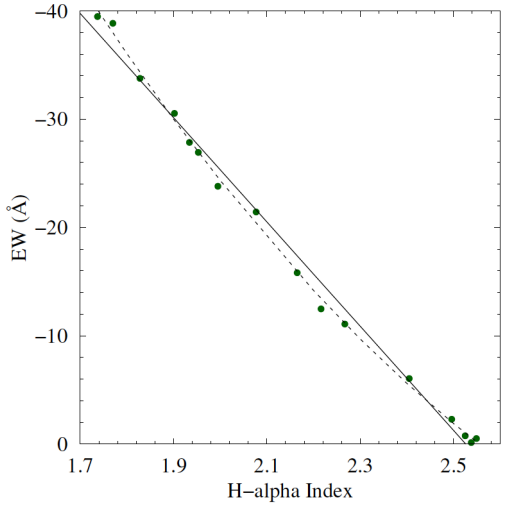

Figure 4. EW width versus Hα index values.

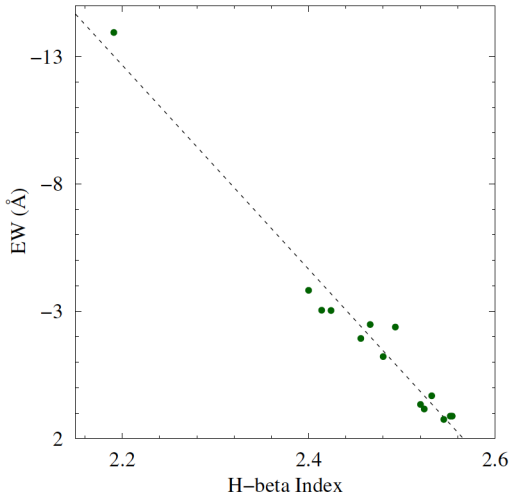

Figure 5. EW width versus Hβ index values.

Table 2. Sample table of Hα and Hβ and equivalent width values for X Per.

HJD	*Hα*	*EWα Å*	*Hβ*	*EWβ Å*
2455261.9115	1.886	–33.0	2.369	–5.9
2455461.9157	1.887	–33.0	2.368	–5.9
2455461.9199	1.886	–33.0	2.370	–5.8
2455548.7535	1.911	–31.5	2.383	–5.3
2455548.7562	1.914	–31.4	2.383	–5.3
2455548.7589	1.913	–31.4	2.382	–5.4
2455611.6519	1.967	–28.4	2.417	–4.0
2455611.6546	1.962	–28.6	2.416	–4.0
2455611.6574	1.958	–28.9	2.407	–4.4
2455612.6251	1.968	–28.3	2.415	–4.0

Note: The remainder of the table is published as a machine-readable table. This table will be web-archived and made available through the AAVSO ftp site at: ftp://ftp.aavso.org/public/datasets/3847-Harding-512-HardingTable2.txt.

Table 3. Sample table of Hα and Hβ and equivalent width values for γ Cas.

HJD	*Hα*	*EWα Å*	*Hβ*	*EWβ Å*
2455806.9621	1.964	–28.5	2.376	–5.6
2455806.9626	1.944	–29.7	2.387	–5.2
2455806.9630	1.905	–31.9	2.405	–4.4
2455828.8716	1.899	–32.2	2.458	–2.3
2455828.8721	1.881	–33.3	2.451	–2.6
2455828.8726	1.892	–32.7	2.429	–3.5
2455904.6018	1.900	–32.2	2.411	–4.2
2455904.6022	1.897	–32.4	2.418	–3.9
2455904.6026	1.901	–32.1	2.414	–4.1
2455904.6029	1.896	–32.4	2.418	–3.9

Note: The remainder of the table is published as a machine-readable table. This table will be web-archived and made available through the AAVSO ftp site at: ftp://ftp.aavso.org/public/datasets/3847-Harding-512-HardingTable3.txt.

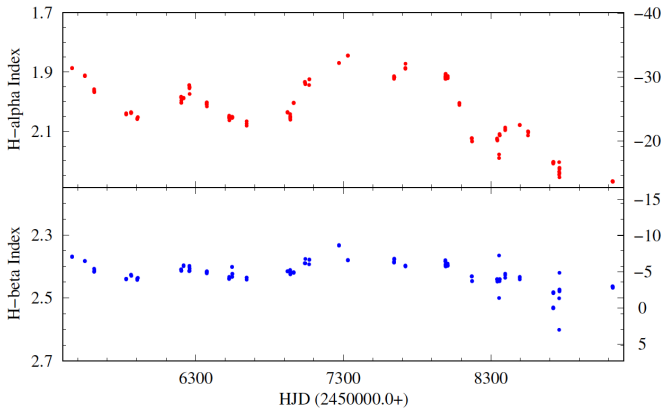

Figure 6. Hα and Hβ values in both index value and equivalent width for X Per. This data covers the time from 2010 to 2020.

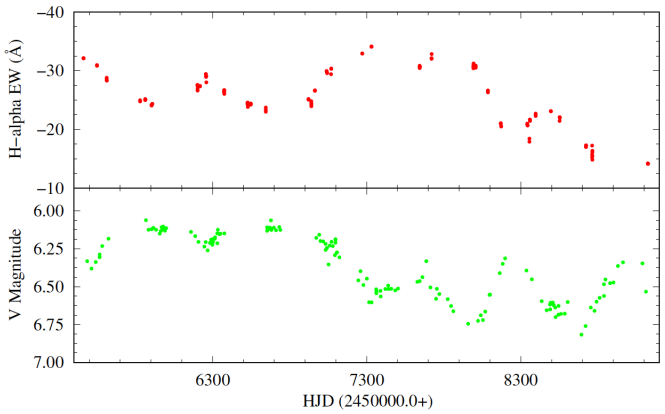

Figure 7. Hα Equivalent Width and V magnitude for X Per over the entire observing time.

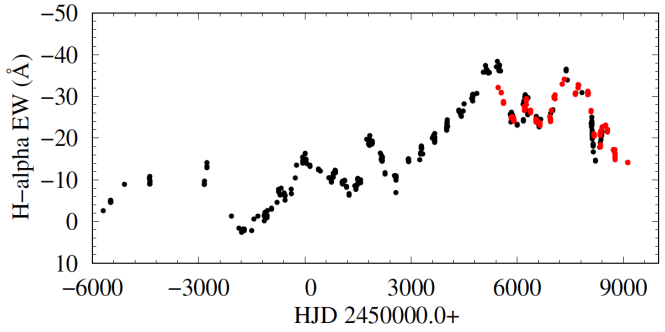

Figure 8. Hα Equivalent Width values with published data (black) and data from this paper (red) for X Persei.

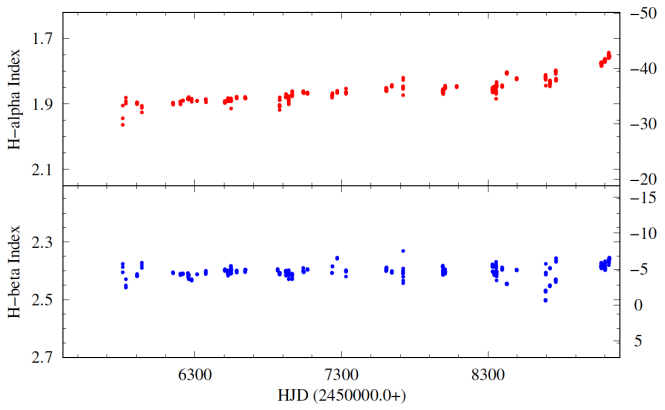

Figure 9. Collected data points of Hα strength of γ Cas during the years 2011 to 2020.

the time range of our data. Minimizing the offset between the two sets of data, at common epochs, we find a systematic shift of –2.2 Å between our values and the published values for the Hα EW. The shift likely comes from differences in how our EW values were determined compared to the published values, including determination of the continuum level. The additional shift is included in the Hα values detailed in Table 2 for X Per and Table 3 for γ Cas to bring them in line with the published values. The systematic shift has not been added to the Hα transformation equation.

3.1. X Persei

In Figure 6 we see the run of both the Hα and Hβ indices for X Per over the time of observation. The scale on the left of the figure is the index values defined by Joner and Hintz (2015) and the right side is the EW in Å. There is clearly a larger range in the Hα line, but the Hβ values do track roughly with the Hα. In all cases the lower, or more negative the value the stronger the hydrogen line. One can clearly see changes in X Per that at first glance might seem periodic in nature, although no periodic nature has ever been confirmed.

A comparison of the Hα values to the published V magnitudes is shown in Figure 7. It is interesting to note that the two curves are almost mirror images of each other: when the V magnitude goes up the strength of the Hα line tends to decrease, although there is not a perfect correspondence.

In Figure 8 we show the published EW values for X Per in black and our data in red. There are clearly a few epochs where our data fill gaps in the overall published curve. To examine the entire run of data for periodic behavior we used the Peranzo software package. Peranzo (Paunzen and Vanmunster 2016) is a package that brings together versions of many standard period search programs like PDM, ANOVA, etc. It includes seven versions of Fourier period searches and nine other methods. We used all 16 packages to examine the combined Hα data for periodic behavior. No clear periodicity was found in any package, as expected.

3.2. γ Cassiopeiae

Following a similar pattern to our X Per analysis, we examined the Hα and Hβ information gathered for γ Cas. In Figure 9 we show the Hα and Hβ variations in our line measurements. γ Cas shows smooth, slowly rising EW values in the Hα index from 2011 to 2020. This is also seen in the data from Pollmann (2021). Our data appear to be in reasonable agreement with the data displayed in that publication. Our Hβ data might show a very small rise over the entire data run, but it is not statistically significant.

4. Conclusions

Using the system detailed in Joner and Hintz (2015) we tracked Hα and Hβ index values over approximately 10 years for X Per and γ Cas. X Per showed significant variations in the Hα index and to a lesser degree in Hβ. γ Cas shows a steady strengthening in the Hα index, with no clear change in Hβ. From the observations of these two objects it is clear that the Hα and Hβ indices can be used to monitor emission-line objects. This

is especially important when the indices are determined from the traditional physical filters.

While future photometric monitoring with the Hα and Hβ indices can be done, it is important to be able to convert to EW values in order to compare with the long range monitoring of these objects. Therefore we provide a conversion between the two indices and EW values. Once converted the EW values determined from the index values agree with published EW.

5. Acknowledgements

Based on observations obtained at the Dominion Astrophysical Observatory, NRC Herzberg, Programs in Astronomy and Astrophysics, National Research Council of Canada. We are especially thankful to David Bohlender and Dmitry Monin at DAO for help with the robotic operations mode. We acknowledge with thanks the variable star observations from the AAVSO International Database contributed by observers worldwide and used in this research. We acknowledge the Brigham Young University, Department of Physics and Astronomy for their continued support of our research efforts. Finally, we acknowledge the help of Maureen Hintz with editorial reviews of all manuscripts.

References

Bugg, A. G., and Hintz, E. G. 2019, *Res. Notes Amer. Astron. Soc.*, **3**, 63.

Crawford, D. L. 1960, *Astrophys. J.*, **132**, 66.

Engin, S., and Yuce, K. 1998, *Inf. Bull. Var. Stars*, No. 4648, 1.

Grundstrom, E. D., *et al.* 2007, *Astrophys. J.*, **660**, 1398.

Joner, M. D., and Hintz, E. G. 2015, *Astron. J.*, **150**, 204.

Kafka, S. 2021, Observations from the AAVSO International Database (https://www.aavso.org/data-download).

Li, H., Yan, J., Zhou, J., and Liu, Q. 2014, *Astron. J.*, **148**, 113.

Liu, Q.-Z. and Hang, H.-R. 2001, *Astrophys. Space Sci.*, **275**, 401.

Paunzen, E., and Vanmunster, T. 2016, *Astron. Nachr.*, **337**, 239.

Pollmann, E. 2021, *J. Amer. Assoc. Var. Star Obs.*, **49**, 77.

Reig, P., Nersesian, A., Zezas, A. 2016, Gkouvelis, L., and Coe, M. J. 2016, *Astron. Astrophys.*, **590A**, 122.

Roche, P., *et al.* 1993, *Astron. Astrophys.*, **270**, 122.

Zamanov, R., Stoyanov, K. A., Wolter, U., Marchev, D., and Petrov, N. I. 2019, *Astron. Astrophys.*, **622A**, 173.